Structure Elucidation

DOI: 10.1002/ange.201407376

Switchable Amplification of Vibrational Circular Dichroism as a Probe of Local Chiral Structure**

Sérgio R. Domingos, Hans J. Sanders, František Hartl, Wybren J. Buma,* and Sander Woutersen**

Abstract: *A new method to detect the vibrational circular dichroism (VCD) of a localized part of a chiral molecular system is reported. A local VCD amplifier was implemented, and the distance dependence of the amplification was investigated in a series of peptides. The results indicate a characteristic distance of 2.0 ± 0.3 bonds, which suggests that the amplification is a localized phenomenon. The amplifier can be covalently coupled to a specific part of a molecule, and can be switched ON and OFF electrochemically. By subtracting the VCD spectra obtained when the amplifier is in the ON and OFF states, the VCD of the local environment of the amplifier can be separated from the total VCD spectrum. Switchable local VCD amplification thus makes it possible to "zoom in" on a specific part of a chiral molecule.*

In most (bio)molecular systems, the functionality is related to a spatially restricted region of the molecule, such as the active site of an enzyme. A detailed understanding of the relation between molecular structure and functionality thus requires the ability to zoom in on that specific part of the system. Ideally, one would like to place a molecular beacon at any specific location in a molecular system so as to "illuminate" only that specific environment. Vibrational circular dichroism (VCD), the circular dichroism associated with vibrational transitions of chiral molecules, is intrinsically capable of probing the spatial structure and conformational changes of molecules in solution. Consequently, in the last two decades, VCD has emerged as a powerful analytical method for absolute-structure determination.[1–20] However, as all parts of the molecule contribute to the VCD spectrum, band overlap often results in congested spectra with limited information regarding specific normal modes. To address this problem, we demonstrate here the implementation of a local VCD amplifier, which can 1) be covalently bound to a specific part of a molecule and 2) be switched on and off electrochemically to provide VCD enhancement in a spatially restricted part of the target molecule.

Recent investigations have shown VCD signal enhancements of more than two orders of magnitude when electronically excited states were strongly coupled to the vibrational manifold of the molecules. The theoretical foundations of the amplification effect have been described in detail elsewhere[21,22] and experimentally confirmed in recent studies.[23–26] We use this effect to locally enhance the VCD of a specific part of a molecule. We investigate the distance dependence of the amplified VCD response in a systematic way using an electroactive moiety that is covalently coupled to a chosen location in a series of peptides using simple chemistry.[27] With this approach, we are able to switch the amplifying source ON and OFF simply by adjusting the electrochemical potential, and we can locally amplify the VCD response. By subtracting the VCD spectra in the ON and OFF states, it is possible to isolate the VCD response of the local environment from the total VCD spectrum. We believe that this approach might ultimately lead to the development of a chirality-sensitive probe with which local effects, such as drug–receptor interactions,[28] biosensing key–lock mechanisms,[29–31] and active sites in proteins and enzymes,[32] can be investigated.

As a first step in this direction, we used an optically transparent thin-layer electrochemical (OTTLE) VCD setup[33] to study the VCD response of a series of peptides that were covalently bound to an electrochemically switchable VCD amplifier. For this specific purpose, we chose ferrocene (Fc) as the external VCD amplifier. In its neutral Fe^{2+} form, ferrocene has a closed-shell electronic configuration with electronically excited states well separated from the electronic ground state. In contrast, the one-electron-oxidized ferrocenium cation has an open-shell configuration (Fe^{3+}) with low-lying electronically excited states, which strongly enhance VCD.[34] The electroactive group can be electrochemically switched ON (open shell) and OFF (closed shell), thus providing a handle for controlled manipulation of the magnitude of the VCD response. An understanding of the spatial sensitivity of the VCD amplification effect is required to predict which molecular entities will be influenced most upon activation of the redox switch. We thus investigated the distance dependence of the VCD amplification in backbone amide I vibrational modes of ferrocenyl-based peptides using VCD spectroelectrochemistry.[33] The relative ease with which this unit can be incorporated at specific locations within

[*] Dr. S. R. Domingos, M. Sc. H. J. Sanders, Prof. Dr. W. J. Buma, Prof. Dr. S. Woutersen
Molecular Photonics Group, Van 't Hoff Institute for Molecular Sciences, University of Amsterdam
Science Park 904, 1098 XH Amsterdam (The Netherlands)
E-mail: w.j.buma@uva.nl
s.woutersen@uva.nl
Prof. Dr. F. Hartl
Department of Chemistry, University of Reading
Whiteknights, Reading RG6 6AD (UK)
E-mail: f.hartl@reading.ac.uk

[**] S.R.D. acknowledges financial support from the Portuguese Foundation for Science and Technology (FCT; SFRH/BD/48295/2008). S.W. would like to acknowledge the European Research Council (ERC) for funding (210999).

Supporting information for this article is available on the WWW under http://dx.doi.org/10.1002/anie.201407376.

a larger molecular system makes it well suited for probing local structure with VCD.

Hereinafter, the designations OFF and ON will be used to describe the two relevant electronic configurations of the electroactive group (ferrocenyl, Fc). We will thus refer to ferrocene in its neutral closed-shell configuration (Fe^{2+}, singlet, no unpaired electrons) as the OFF configuration, whereas the oxidized, cationic open-shell configuration (Fe^{3+}, doublet, one unpaired electron) will be referred to as the ON configuration. The ON configuration generates an electronic manifold with low-energy electronically excited states, that is, it "activates" the VCD amplification, whereas the OFF configuration turns off the amplification by returning the electronic manifold to its original configuration, without low-lying electronically excited states.

In Figure 1 (right), we show the molecular structure of the first prototype, a ferrocene moiety that is connected to the L-Ala-L-Ala methyl ester (Fc-(L)-Ala-Ala). The chemical groups that serve as a probe for the spatial extent of the VCD enhancement are labeled based on their increasing distance from the electroactive group and referenced by the ruler plotted next to the molecular structure as a guide to the eye. Figure 1 A (left) shows infrared absorption spectra of Fc-(L)-Ala-Ala in the OFF (solid line) and ON (dashed line) configurations. We can promptly assign three vibrational modes, which are labeled according to their positions as displayed in Figure 1 (right). In the OFF configuration, there are two amide I vibrational modes (1 and 2) at 1650 and 1684 cm^{-1}, respectively. Band 3 at higher frequency (ca. 1750 cm^{-1}) are due to the methyl ester C=O stretching. Upon electrochemical switching to the ON configuration, the frequency of amide-I mode 1 increases by 19 cm^{-1}, while the frequency of amide-I mode 2 increases by only 3.5 cm^{-1}. The C=O methyl ester vibrational mode (3) does not undergo any frequency shift (see Table 1). Our spectral window shows well-separated bands for the vibrational modes under investigation, thus allowing for a clear comparison of VCD intensities (Figure 1).

Table 1: Frequency shifts and anisotropy factors ($g = \Delta\varepsilon/\varepsilon$) for the vibrational modes 1, 2, and 3 in the OFF and ON configurations of Fc-(L)-Ala-Ala.

		OFF			ON		
Mode	$\Delta\nu$ [cm^{-1}]	ε	$\Delta\varepsilon$	g	ε'	$\Delta\varepsilon'$	g'
1	19.0	1024	0.01	9.7×10^{-6}	1380	0.10	7.2×10^{-5}
2	3.5	820	0.02	2.4×10^{-5}	840	0.05	5.9×10^{-5}
3	0	640	0.01	1.6×10^{-5}	650	NA	NA

NA = not applicable.

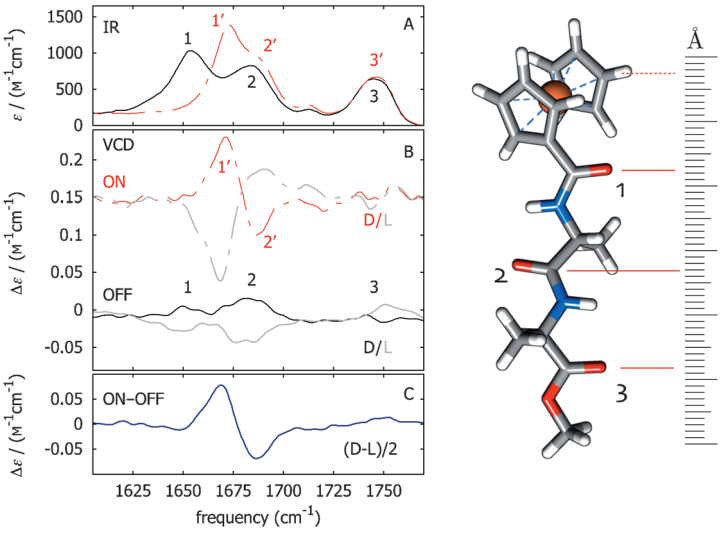

Figure 1. Left: A, B) Infrared absorption (A) and VCD spectra (B) of the Fc-(L/D)-Ala-Ala ester (10^{-2} M) in CD_3CN (10^{-1} M Bu_4NPF_6, 200 μm optical path length). The VCD spectra of the ON configuration are offset for clarity. C) Difference spectrum of the VCD spectra in the ON and OFF configurations. Right: Molecular structure of Fc-(L)-Ala-Ala. A ruler is shown next to the peptide backbone to highlight the distance between the ferrocene moiety and the amide and ester groups.

Figure 1 B displays the VCD spectra for the OFF/ON configurations. Comparison of the VCD signal intensities for vibrational modes 1, 2, and 3 (OFF) and the corresponding modes 1′, 2′, and 3′ (ON) readily shows the amplified VCD response in the ON configuration. As a direct measure of the amplification magnitudes we used the anisotropy factors $g = \Delta\varepsilon/\varepsilon$ of each vibrational mode. The results reported in Table 1 indicate that the signal intensity of the amide I (Ala_1) vibration was amplified most, whereas the amide I (Ala_2) signal was only slightly enhanced (the C=O methyl ester (Ala_3) VCD intensity lies within the noise of the measurement and therefore cannot be evaluated accurately). The amplification thus seems to be stronger for the amide I mode closest to the ferrocene moiety than for the other amide I and the C=O methyl ester modes. In Figure 1 C, the ON–OFF difference spectrum is shown. As the intensities of the bands in the VCD spectrum of the system in the ON configuration are strongly dependent on the distance from the amplifying unit, this spectrum "zooms in" on the part of the system that is within the amplification range.

The above observations indicate that the normal modes close to the ferrocene are most prone to VCD enhancement. We extended the probing range to gain further insight into the distance dependence of the VCD enhancement. To this purpose, we compared the amplification factors of the VCD signals in a tripeptide (Ala-Pro-Ala) attached to ferrocene, see Figure 2 (right) for the molecular structure. Ala-Pro-Ala was specifically chosen for this study because of its well-separated amide I frequencies, allowing us to separate the VCD bands for better evaluation of signal intensity and amplification. The proline residue has a distinct red-shifted amide I vibrational frequency compared to that of alanine. Moreover, the electron-withdrawing character of the amide functional group in Ala_1 leads to distinct amide I frequencies for the two alanine moieties. Figure 2 A shows the infrared absorption spectrum of Fc-(L)-Ala-Pro-Ala (OFF configuration), which shows three amide I modes (Ala_1, Pro_2, and Ala_3) and one methyl

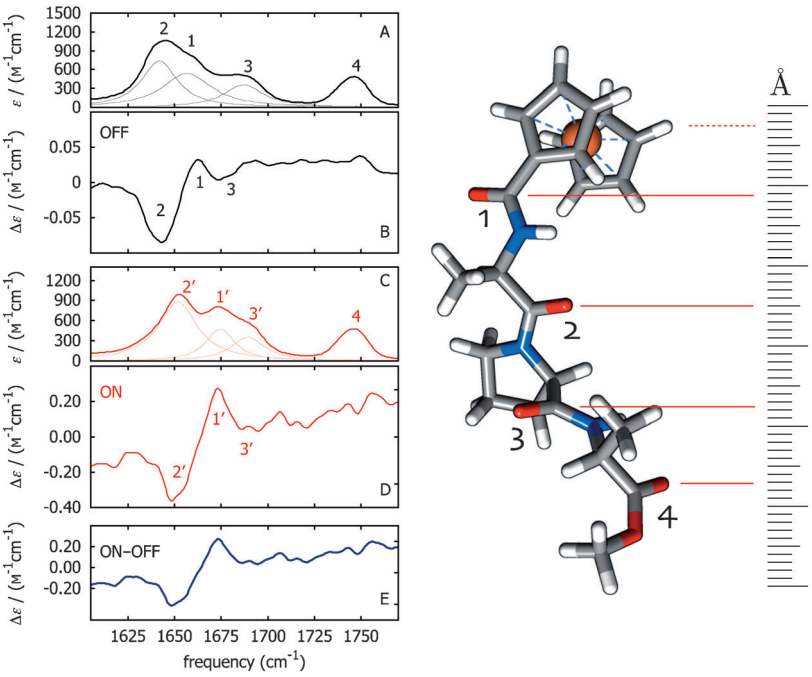

Figure 2. Left: A–D) Infrared absorption (A, C) and VCD spectra (B, D) of Fc-(L)-Ala-Pro-Ala (10^{-2} M) in CD_3CN (10^{-1} M Bu_4NPF_6, 200 μm optical path length) for the OFF and ON configurations, respectively. E) Difference spectrum of the VCD spectra in the ON and OFF configurations. Right: Molecular structure of Fc-(L)-Ala-Pro-Ala. A ruler is shown next to the peptide backbone to highlight the distance between the ferrocene moiety and the amide and ester groups.

ester C=O stretching mode (Ala_4) in the spectral window. As expected, all three modes have distinct frequencies as evidenced by the Lorentzian curves that fit the FTIR spectrum. We assigned the frequencies of the four modes as follows: Pro_2 (1642 cm^{-1}), Ala_1 (1657 cm^{-1}), Ala_3 (1687 cm^{-1}), and Ala_4 (1745 cm^{-1}). The subscripts correspond to the numbered positions in Figure 2 (right). In Figure 2B, we show the VCD spectrum of Fc-(L)-Ala-Pro-Ala with ferrocene in the OFF configuration. Three features are readily identified in the spectrum and assigned according to the numbering in Figures 2A. The molar absorption coefficients (ε) and the differential absorption coefficients ($\Delta\varepsilon$) are listed in Table 2.

The infrared absorption and VCD spectra of Fc-(L)-Ala-Pro-Ala in the ON configuration are shown in Figure 2C,D. All of the infrared bands were blue-shifted except for Ala_4 (see Table 2), although the modes were not equally affected by the oxidation of the ferrocenyl moiety (Table 2). As expected, the overall VCD signal intensities (Figure 2D) were considerably enhanced compared with those of the bands in the OFF configuration. Figure 2E displays the ON–OFF difference VCD spectrum. We find that the signals from normal modes 3 and 4 are suppressed, and that the amplifying unit again zooms in on the nearby normal modes 1 and 2. However, the amplification factors for the individual modes differ considerably. Again, to accurately compare the intensity enhancements for each mode, we determined their anisotropy factors ($g = \Delta\varepsilon/\varepsilon$) in the OFF and ON configurations. In Figure 3, the amplification factor, defined as the ratio g'/g, was plotted as a function of the distance of the normal mode to the electroactive moiety for Fc-(L)-Ala-Ala and Fc-(L)-Ala-Pro-Ala. The correlation between g'/g and the distance of the amide groups from the Fc moiety provides clear evidence that the enhancement decays strongly with increasing distance from the amplifier.

To quantify the spatial extent of the amplification we have performed a fit to the data points in Figure 3 to the function $1+A\,e^{-x/R_0}$, where the variable x represents the distance (in number of bonds) between the chemical group and the amplifying center. From the fit we obtain a characteristic distance R_0 of 2.0 ± 0.3 bonds, that is, the VCD amplification is reduced by a factor of 1/e for a chemical group that is at a distance of two bonds from the amplifying center. This characteristic distance may be different for other types of compounds and other types of bonds, for example, in conjugated double bonds or in bonds with different spatial orientation.

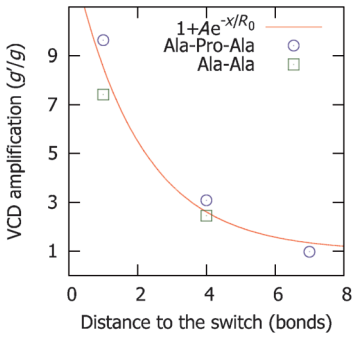

Figure 3. VCD amplification factors (g'/g) as a function of the distance (number of covalent bonds) from the electroactive group to each of the indicated functional groups of Fc-(L)-Ala-Ala and Fc-(L)-Ala-Pro-Ala.

Table 2: Frequency shifts and anisotropy factors ($g = \Delta\varepsilon/\varepsilon$) for the vibrational modes 1, 2, 3, and 4 in the OFF and ON configurations of Fc-(L)-Ala-Pro-Ala.

		OFF			ON		
Mode	$\Delta\nu$ [cm^{-1}]	ε	$\Delta\varepsilon$	g	ε'	$\Delta\varepsilon'$	g'
1	17.84	534	0.03	5.6×10^{-5}	476	0.26	5.4×10^{-4}
2	9.88	738	0.07	9.4×10^{-5}	875	0.26	2.9×10^{-4}
3	2.32	348	0.02	5.7×10^{-5}	354	0.02	5.6×10^{-5}
4	0	483	NA	NA	478	NA	NA

NA = not applicable.

To conclude, we have shown how amplified vibrational circular dichroism can be used to zoom in on specific parts of biomolecular systems. To this purpose, we have investigated ferrocenyl-substituted

peptides, which are prototypical examples of how a switchable amplifying unit (ferrocene) can be incorporated into a larger structure, such as a protein. In the OFF configuration, no amplification occurs, whereas in the ON configuration, low-energy excited states are present that enhance the VCD by more than one order of magnitude. The observed distance dependence of the VCD enhancement along the peptide backbone shows that the amplification is a localized phenomenon. Hence, the ON–OFF VCD difference spectrum is exclusively sensitive to the chiral structure in the direct neighborhood of the amplifier, whereas the signals from normal modes that are further removed from the amplifier are eliminated. Switchable VCD amplification thus provides a unique method to determine local chiral structure in complex (bio)molecular systems.

Received: July 18, 2014
Published online: September 11, 2014

Keywords: chirality · circular dichroism · local probes · peptides · structure elucidation

[1] L. A. Nafie, *Vibrational Optical Activity*, Wiley, Chichester, **2011**.
[2] L. A. Nafie, T. A. Keiderling, P. J. Stephens, *J. Am. Chem. Soc.* **1976**, *98*, 2715 – 2723.
[3] P. L. Polavarapu, C. Zhao, *J. Anal. Chem.* **2000**, *366*, 727 – 734.
[4] T. A. Keiderling, P. J. Stephens, *J. Am. Chem. Soc.* **1977**, *99*, 24.
[5] A. T. Krummel, M. T. Zanni, *J. Phys. Chem. B* **2006**, *110*, 24720 – 24727.
[6] V. Andrushchenko, D. Tsankov, M. Krasteva, H. Wieser, P. Bour, *J. Am. Chem. Soc.* **2011**, *133*, 15055 – 15064.
[7] S. L. Ma, X. L. Cao, M. Mak, A. Sadik, C. Walker, T. B. Freedman, I. K. Lednev, R. K. Dukor, L. A. Nafie, *J. Am. Chem. Soc.* **2007**, *129*, 12364.
[8] T. J. Measey, K. B. Smith, S. M. Decatur, L. M. Zhao, G. L. Yang, R. Schweitzer-Stenner, *J. Am. Chem. Soc.* **2009**, *131*, 18218.
[9] D. Kurouski, R. A. Lombardi, R. K. Dukor, I. K. Lednev, L. A. Nafie, *Chem. Commun.* **2010**, *46*, 7154 – 7156.
[10] T. J. Measey, R. Schweitzer-Stenner, *J. Am. Chem. Soc.* **2011**, *133*, 1066 – 1076.
[11] A. Fulara, A. Lakhani, S. Wojcik, H. Nieznanska, T. A. Keiderling, W. Dzwolak, *J. Phys. Chem. B* **2011**, *115*, 11010 – 11016.
[12] D. Kurouski, K. Kar, R. Wetzel, R. K. Dukor, I. K. Lednev, L. A. Nafie, *FEBS Lett.* **2013**, *587*, 1638 – 1643.
[13] R. A. G. D. Silva, J. Kubelka, P. Bour, S. M. Decatur, T. A. Keiderling, *Proc. Natl. Acad. Sci. USA* **2000**, *97*, 8318 – 8323.
[14] P. Zhu, G. Yang, M. R. Poopari, Z. Bie, Y. Xu, *ChemPhysChem* **2012**, *13*, 1272 – 1281.
[15] F. Eker, X. Cao, L. Nafie, R. Schweitzer-Stenner, *J. Am. Chem. Soc.* **2002**, *124*, 14330 – 14341.
[16] X. Li, K. H. Hopmann, J. Hudecova, W. Stensen, J. Novotna, M. Urbanova, J.-S. Svendsen, P. Bour, K. Ruud, *J. Phys. Chem. A* **2012**, *116*, 2554 – 2563.
[17] H. Sato, T. Taniguchi, A. Nakahashi, K. Monde, A. Yamagishi, *Inorg. Chem.* **2007**, *46*, 6755 – 6766.
[18] S. R. Domingos, S. J. Roeters, S. Amirjalayer, Z. Yu, S. Hecht, S. Woutersen, *Phys. Chem. Chem. Phys.* **2013**, *15*, 17263 – 17267.
[19] R. Schweitzer-Stenner, F. Eker, K. Griebenow, X. Cao, L. A. Nafie, *J. Am. Chem. Soc.* **2004**, *126*, 2768 – 2776.
[20] R. Schweitzer-Stenner, *J. Phys. Chem. B* **2004**, *108*, 16965.
[21] L. A. Nafie, T. B. Freedman, *J. Chem. Phys.* **1983**, *78*, 7108.
[22] L. A. Nafie, *J. Phys. Chem. A* **2004**, *108*, 7222 – 7231.
[23] S. R. Domingos, A. Huerta-Viga, L. Baij, S. Amirjalayer, D. A. E. Dunnebier, A. J. C. Walters, M. Finger, L. A. Nafie, B. de Bruin, W. J. Buma, S. Woutersen, *J. Am. Chem. Soc.* **2014**, *136*, 3530 – 3535.
[24] S. R. Domingos, M. R. Panman, B. H. Bakker, F. Hartl, W. J. Buma, S. Woutersen, *Chem. Commun.* **2012**, *48*, 353 – 355.
[25] C. Johannessen, P. W. Thulstrup, *Dalton Trans.* **2007**, 1028 – 1033.
[26] Y. He, X. Cao, L. A. Nafie, T. B. Freedman, *J. Am. Chem. Soc.* **2001**, *123*, 11320 – 11321.
[27] E. Valeur, M. Bradley, *Chem. Soc. Rev.* **2009**, *38*, 606 – 631.
[28] L. J. Parker, D. B. Ascher, C. Gao, L. A. Miles, H. H. Harris, M. W. Parker, *J. Inorg. Biochem.* **2012**, *115*, 138 – 147.
[29] B. Lal, A. Badshah, A. A. Altaf, N. Khan, S. Ullah, *Appl. Organomet. Chem.* **2011**, *25*, 843 – 855.
[30] S. Martić, M. Labib, P. O. Shipman, H.-B. Kraatz, *Dalton Trans.* **2011**, *40*, 7264 – 7290.
[31] R. Trivedi, S. B. Deepthi, L. Giribabu, B. Sridhar, P. Sujitha, C. G. Kumar, K. V. S. Ramakrishna, *Appl. Organomet. Chem.* **2012**, *26*, 369 – 376.
[32] S. Mitra, R. C. Holz, *J. Biol. Chem.* **2007**, *282*, 7397 – 7404.
[33] S. R. Domingos, H. Luyten, F. van Anrooij, H. J. Sanders, B. H. Bakker, W. J. Buma, F. Hartl, S. Woutersen, *Rev. Sci. Instrum.* **2013**, *84*, 033103.
[34] Y. S. Sohn, D. N. Hendrickson, H. B. Gray, *J. Am. Chem. Soc.* **1971**, *93*, 3603 – 3612.

